

Intrinsic glue distribution at very small x

Jamal Jalilian-Marian, Alex Kovner, Larry McLerran, and Heribert Weigert

Physics Department, University of Minnesota, 116 Church Street S.E., Minneapolis, Minnesota 55455

(Received 6 August 1996)

We compute the distribution functions for gluons at very small x and not too large values of transverse momenta. We extend the McLerran-Venugopalan model by using renormalization group methods to integrate out effects due to those gluons which generate an effective classical charge density for Weizsäcker-Williams fields. We argue that this model can be extended from the description of nuclei at small x to the description of hadrons at yet smaller values of x . This generates a Lipatov-like enhancement for the intrinsic gluon distribution function and a nontrivial transverse momentum dependence as well. We estimate the transverse momentum dependence for the distribution functions, and show how the issue of unitarity is resolved in lepton-nucleus interactions. [S0556-2821(97)05407-6]

PACS number(s): 12.38.Bx, 12.38.Mh, 24.85.+p, 25.75.Dw

I. INTRODUCTION

The problem of computing the distribution functions for gluons at very small x is an old one [1]. The gluon (and quark) distribution functions are computable in perturbation theory at large values of x , but at small x one encounters a so-called Lipatov enhancement. The precise computation of this enhancement is subject to much uncertainty, primarily because at some point in the evolution the density of gluons becomes so large that there are mutual interactions of the gluons which are ignored in the Balitskii-Fadin-Kuraev-Lipatov (BFKL) equation. In addition, the behavior at small x also involves knowing the distribution function at small Q^2 , and again nonperturbative information seems to be needed.

Recently, a different framework was advocated for the computation of the gluon distribution functions [2]. The starting point of this approach is to view a hadron not as a collection of a small number of partons, but rather as a system with finite parton density. In the high density situation, the natural way to describe the soft gluons is not as quasifree particles, but as classical fields with a large amplitude. These classical fields are generated by classical color charges which represent the valence partons. Once the high density effects are resummed into the classical fields, one may apply weak coupling methods to calculate quantum corrections. In this approach, high gluon densities which prove so problematic in the BFKL context are a prerequisite for the description of the parton content of a nucleus wave function via classical gluon fields.

A consistent separation in field and particlelike degrees of freedom can be performed most easily in the infinite momentum frame. The object of computation is the intrinsic x and p_\perp contributions to the infinite momentum hadronic wave function in the light cone gauge. Distribution functions are given as

$$Q[x, Q^2] = \int_0^{Q^2} d^2 p_\perp \frac{dN}{dx d^2 p_\perp} \quad (1)$$

in terms of the intrinsic parton distributions as computed by taking the expectation value of the number operator in the state of interest.

In the infinite momentum frame, the valence partons are strongly Lorentz contracted. If we then look for spread-out gluon fields at $x \ll A^{-1/3}$, interactions between valence partons and soft gluon fields eikonalize, which indeed allows us to take the particle limit for the fast-moving partons. Here A is the baryon number of a nucleus. For a hadron, $x \ll 1$. The hadron will indeed appear as an infinitesimally thin sheet on the scale of wavelengths associated with the momentum fraction x . (We will later see that we will have to regularize this source by giving it a large but finite momentum and a longitudinal extent of order R/γ where R is its size in the rest frame and γ is its Lorentz gamma factor. We will find that nothing in leading order of our computations depends upon the details of this regularization.) In addition, for a thick nucleus, since the number of sources of charge per unit area scales as $A^{1/3}$, we may view the valence partons (quarks) as classical color charges. Therefore, somewhat paradoxically, the simplest problem to start with is computing the gluon distributions for a very large nucleus.

We will find later that at very small x the glue as well as valence quarks contributes to the charge density seen by a gluon. The gluons which contribute to the charge density are all gluons with an x larger than the x of the gluon whose structure function is being measured. Therefore the consideration discussed above for nuclei will apply to hadrons when at sufficiently small x so that the number of gluons at larger values of x is large. The advantage of nuclei is that large densities of charge are generated at larger values of x , and therefore lower energy per nucleon, than is the case for a single hadron.

A solution of this problem would be useful in a variety of contexts. The approach we advocate involves knowledge of the nuclear wave function and is somewhat related to the approach of Mueller for heavy quarkonia [3]. Our approach in principle allows the resolution of various phenomenological problems which arise in the parton cascade model of particle production in heavy ion collisions [4]. These models provide the initial condition for hydrodynamic calculations [5]. A model which builds in the space-time structure we advocate and uses the information we have generated for the infinite momentum frame wave functions is given in Ref. [6].

The theory which results at the classical level is basically a Yang-Mills theory in the presence of a source:

$$J_a^+ = \delta(x^-) \rho_a(x_\perp). \quad (2)$$

The measure which generates the expectation values of gluon fields, corresponding to distribution functions, is

$$\int [dA][d\rho] \exp\left(-\int d^2x_\perp \frac{1}{\mu^2} \text{Tr}\rho^2(x_\perp)\right) \exp(iS), \quad (3)$$

where S is the ordinary gluon action in the presence of the external current J . The parameter μ^2 is the valence color charge per unit area [scaled by a factor $1/(N_c^2-1)$]. In leading order, the expectation value is given by a classical field which is a solution of the Yang-Mills equation¹

$$D_\mu F^{\mu\nu} = g^2 J^\nu, \quad (4)$$

which is then averaged over different values of ρ .

In the limit where the gluon field generated by these valence quarks is treated classically, the gluon field is a non-Abelian Weizsäcker-Williams field and has the form

$$A^+ = A^- = 0 \quad (5)$$

and

$$A^i = \theta(x^-) \alpha^i(x_\perp). \quad (6)$$

The field $\alpha^i S$ is a two-dimensional ‘‘pure gauge’’

$$\alpha^i = -\frac{1}{i} U \nabla^i U^\dagger. \quad (7)$$

The physical justification for the non-Abelian Weizsäcker-Williams field is that because the source of charge is confined to a thin sheet, the solution must solve the free equations of motion everywhere but on the sheet. The solution is therefore a gauge transform of zero field on either side of the sheet. The discontinuity of the fields across the sheet gives the charge density.

It was suggested by McLerran and Venugopalan that this simple model should give a decent approximation for the soft glue distribution function. It turns out, however, that the corrections to the distribution function calculated in this way are large at small x . Technically, there are two sources for these corrections, although both have the same physical origin.

First, as we will show, the behavior of the correlation function calculated in this simple-minded approach is singular at small p_\perp . The flaw in the treatment of Ref. [2] was that the source of charge was not treated as an extended distribution which tends to a δ function only in the infinite momentum limit [8,9]. Physically, it is clear that the charge density is indeed spread out on the scale of the characteristic longitudinal momentum of the hard particles which generate this density.

The second source of large corrections is basically the same small- x enhancement as in standard perturbative calcu-

lations. As was shown in Ref. [7], the quantum corrections to the distribution functions calculated in terms of the classical fields become large at small x , the enhancement factor being the infamous $\alpha \ln 1/x$.

The main goal of this paper is to show that the two corrections are physically related and to outline a solution to both problems. We will show that the small- x enhancement arises from quantum fluctuations with large longitudinal momentum. We show that such configurations may be successfully integrated out by using renormalization group techniques reminiscent of the Wilson block spin method. This approach can also be interpreted in terms of the adiabatic or Born-Oppenheimer approximation extensively used in atomic physics. Integrating out hard quantum fluctuations is equivalent to including the harder gluons into what we call the charge density ρ in Eq. (3), while calculating the distribution of the softer glue. It therefore leads to ‘‘renormalization’’ of the charge density and endows it with nontrivial and calculable longitudinal structure.

This modified momentum-dependent distribution of source strengths leads to infrared nonsingular correlation functions. We argue that the result is sensitive only to the average charge squared per unit rapidity per unit transverse area of the source.

The outline of this paper is as follows.

In Sec. II, we study the classical problem of computing the fields associated with a source of charge which is extended in x^- . We find the general solution to this problem in the light cone gauge. We compute the resulting distribution functions assuming that the source is random in x_\perp and x^- , but with a weight of charge squared per unit rapidity per unit area, which is specified.

In Sec. III, we show by using the renormalization group techniques how to generate classical fields at some rapidity scale y . This involves perturbatively integrating out modes at larger values of rapidity (smaller values of x^-). This integration generates an effective Lagrangian which has a self-similar form, namely, that at each step of the procedure it is similar to the McLerran-Venugopalan model, but with a charge per unit area which is rapidity dependent. We show that this effective theory is equivalent to that discussed in Sec. II. We derive the renormalization group equations for the charge squared per unit area per unit rapidity as measured at some transverse momentum scale Q^2 and rapidity $y = y_0 + \ln(x_0^-/x^-)$, where y_0 is the nucleus rapidity and $x_0^- \sim R/\gamma$. The calculations in this section rely on several simplifying approximations, which we discuss.

In Sec. IV, we study the renormalization group equations for the charge squared per unit rapidity per unit area as a function of Q^2 and y . This equation is closely related to the usual evolution equations for the distribution function which appear in standard perturbative treatments. It can be viewed as a nonlinear version of the Dokshitzer-Gribov-Lipatov-Altarelli-Parisi (DGLAP) equation. We show that for p_\perp much larger than the momentum scale associated with the charge squared per unit rapidity integrated over all rapidities larger than that at which we measure the structure functions [which we will refer to as $\chi(y, Q^2)$], the nonlinearities in the renormalization group (RG) equation become unimportant. In this regime the equation basically describes the double-logarithmic DGLAP evolution. At lower momenta our equa-

¹For conventions on the use of the coupling constant, see the next section.

tion can be thought of as a nonlinear variant of the BFKL equation, although to make the relation precise one would have to consider some virtual corrections in addition to those accounted for in our derivation. At low transverse momentum, we show that the evolution equation saturates. We discuss the consistency issues which are necessary for a solution of this equation within the set of approximations for which our derivation is valid.

In the final sections we summarize our results. We show how our results are consistent with unitarity in deep inelastic scattering. We estimate the total cross section at fixed Q^2 as x approaches zero. We argue that a computation of the charge squared per unit rapidity per unit area would allow a computation of the total multiplicity in hadronic interactions. We discuss the possible universality of our results and their possible generalization to the description of nucleons at small x . We discuss some of the many problems which are not yet solved within the approach advocated in this paper.

II. MODIFICATION OF THE SOURCE STRENGTH DUE TO EXTENDED STRUCTURE IN x^-

In this paper we will use gauge potentials scaled such that the covariant derivative reads $D_\mu[A] = \partial_\mu - iA_\mu$. The classical gluonic action is of the form $(-1/4g^2)F^2$ and hence a $g^2 J^\mu$ term in the classical equations of motion. In this setup gauge transformations U are most economically parameterized via $U(x) = \exp[i\Lambda(x)]$ transforming A as $A \rightarrow U[A - (1/i)\partial]U^{-1}$. We will be also using matrix notation, e.g., $\rho = \rho^a T^a$, where T^a are the normalized Hermitian generators of the $SU(N_c)$ group in the fundamental representation, $2 \text{Tr} T^a T^b = \delta^{ab}$.

In the original McLerran-Venugopalan approach [2], the source strength was assumed to have the form

$$J_a^+(x^-, x_\perp) = \delta(x^-) \rho_a(x_\perp) \quad (8)$$

and to be distributed with the Gaussian weight

$$\int [d\rho] \exp\left[-\frac{1}{\mu^2} \int d^2x_\perp \text{Tr} \rho^2(x_\perp)\right], \quad (9)$$

where μ^2 is the charge per unit area.

The solutions to the Yang-Mills equation in the $A^+ = 0$ gauge have vanishing A^- . Their transverse components A^i are determined through

$$\nabla_i \partial^+ A^i + [A_i, \partial^+ A^i] = g^2 J^+, \quad (10)$$

together with

$$F^{ij} = 0. \quad (11)$$

It was argued that the solution was of the form

$$A^i(x) = \theta(x^-) \alpha^i(x_\perp). \quad (12)$$

In this solution, the commutator term in Eq. (10) was ignored since it involves the commutator of the field at the same point in x^- .

Ignoring the commutator term is, however, not justified. It is clear that this term in Eq. (10) is very singular and involves a product of $\delta(x^-)$ and $\theta(x^-)$. To make sense of this

structure, we must understand the evolution of the field across the δ function singularity. This can only be done if we know the structure of the source in x^- . In fact, as shown in [8], ignoring this problem leads to infrared singular distributions.

Let us introduce the space-time rapidity variable

$$y = y_0 + \ln(x_0^-/x^-), \quad (13)$$

which will be useful for $x^- > 0$. We will assume that the source strength is nonvanishing only for positive x^- , and we will work in a gauge where the fields A^i vanish for $x^- < 0$. The rapidity y_0 is the momentum space rapidity of the nucleus, and the parameter x_0^- is the typical Lorentz-contracted size of the nucleus, $x_0^- \sim R/\gamma$.

In the next section, we will use renormalization group arguments to show that there is a nontrivial induced source strength extending beyond the volume occupied by valence partons which is driven by gluon modes at longitudinal momentum larger than that at which we measure the gluon distribution. This is parametrized by some strength of charge squared per unit area per unit space-time rapidity $\mu^2(y, Q^2)$ and by the charge per unit area at rapidities greater than y :

$$\chi(y, Q^2) = \int_y^\infty dy' \mu^2(y', Q^2). \quad (14)$$

The parameter Q^2 appears because we must specify at what value of Q^2 we are measuring the distribution function. It has precisely the same meaning as in perturbative QCD calculations, namely, the transverse scale at which a parton is resolved [10]. It should not be confused with the intrinsic transverse momenta of the fields.

Accounting for the space-time rapidity dependence of the source strength, we therefore are led to consider the distribution

$$\int [d\rho] \exp\left[-\int_0^\infty dy \int d^2x_\perp \frac{\text{Tr} \rho^2(y, x_\perp)}{\mu^2(y, Q^2)}\right]. \quad (15)$$

In this equation, ρ is the charge density per unit transverse area per unit space-time rapidity.² In the previous work we took great pain to argue that the charge could be treated classically on transverse scales which are large compared to the density of partons per unit area. This was because on this scale there is a large number of partons contributing to the source, and therefore the charges were in a large dimensional representation of the color group. This allowed a classical treatment.

The longitudinal structure is a new ingredient. Why can we still approximate the partons (gluons) that couple to soft glue by a classical source? The physical reason is easy to understand: For these high momentum gluons, the coupling

²The parameter $\mu^2(y)$ controls the magnitude of the fluctuations of the charge density at fixed rapidity y . Since there is no charge density at rapidities greater than the rapidity of the nucleus y_0 , the function $\mu^2(y)$ should vanish for $y \geq y_0$. The rapidity integrals in Eqs. (14) and (15) are therefore effectively cutoff at this upper limit.

is weak, so that to change the field (the soft glue) by a correction of order 1, one must have many (hard) gluons contributing. In the next section, we will see that the induced source of gluons is in fact slowly varying in rapidity

$$\frac{d^2\rho}{dy^2} \sim \alpha \frac{d\rho}{dy}. \quad (16)$$

Again, we will see this justified in more detail in the next section.

Therefore these sources of charge come from an extended region of space-time rapidity with a typical contribution at a rapidity far greater than that of the field we are computing. The source will therefore appear to be infinitesimally thin in the variable x^- .

We must solve Eq. (10) in the presence of source with a prescribed rapidity dependence. This is best done in terms of the rapidity variable y introduced in Eq. (13). Equation (10) becomes

$$D_i \frac{d}{dy} A^i = g^2 \rho(y, x_\perp). \quad (17)$$

In this equation, because of the extended structure in rapidity, the term which involves the group cross product of two A^i fields cannot be ignored.

The formal solution to this equation can be found by introducing the line-ordered phase

$$U(y, x_\perp) = U_{\infty, y}(x_\perp) = \hat{\mathbf{P}} \exp \left[i \int_y^\infty dy' \Lambda(y', x_\perp) \right], \quad (18)$$

representing a parallel transport operator along a straight line at fixed x^+ and x_\perp connecting y to ∞ ($x^- = 0$). Recall that due to the vanishing of the transverse magnetic field ($F^{ij} = 0$), the vector potential should be a ‘‘two-dimensional pure gauge.’’ We let, therefore,

$$A^i(y, x_\perp) = iU \nabla^i U^{-1}. \quad (19)$$

This leads to the equation for Λ :

$$\nabla^2 \Lambda = -g^2 U^{-1} \rho U. \quad (20)$$

The above equation may be solved directly numerically. Imagine we have a grid in rapidity y and transverse coordinates. We define the lattice spacing in rapidity as a_y . The above equation can be written as

$$\begin{aligned} \nabla^2 \Lambda(y, x_\perp) = & -g^2 \left(\hat{\mathbf{P}} \exp \left[i \int_{y+a_y}^\infty dy' \Lambda(y', x_\perp) \right] \right)^{-1} \\ & \times \rho(y, x_\perp) \left(\hat{\mathbf{P}} \exp \left[i \int_{y+a_y}^\infty dy' \Lambda(y', x_\perp) \right] \right). \end{aligned} \quad (21)$$

The solution at y depends only upon the function Λ at larger values of rapidity. This equation may therefore be solved iteratively starting at some maximum y_{\max} beyond which the source vanishes.

It turns out, however, that we do not need to know an explicit solution in order to calculate the distribution func-

tion. For that, we have to perform the integration over the source strength $\rho(y, x_\perp)$. Let us change the variables in the path integral, Eq. (15), from $\rho(y, x_\perp)$ to $\Lambda(y, x_\perp)$. The Jacobi of this transformation does not depend on ρ . This is easily verified noting that the Jacobian matrix is triangular in y and, as a result of the y orderings involved in the relation between ρ and Λ , has no interactions on the diagonal. We find, therefore, that, for any function $O(\rho)$,

$$\begin{aligned} & \int [d\rho] \exp \left[- \int_0^\infty dy \int d^2x_\perp \frac{\text{Tr} \rho(y, x_\perp)^2}{\mu^2(y, Q^2)} \right] O(\rho) \\ & = \int [d\Lambda] \exp \left[- \int_0^\infty dy \int d^2x_\perp \frac{\text{Tr} [\nabla^2 \Lambda(y, x_\perp)]^2}{g^4 \mu^2(y, Q^2)} \right] Q(\Lambda). \end{aligned} \quad (22)$$

Since the classical fields A_i are given as explicit functions of Λ and our aim is to compute the distribution function

$$G_{ij}(y, x_\perp; y', x'_\perp) = \langle A_i(y, x_\perp) A_j(y', x'_\perp) \rangle, \quad (23)$$

this form of the path integral is very convenient.

We first note that

$$A^i(y, x_\perp) = \int_y^\infty dy' U_{\infty, y'}(x_\perp) (\nabla^i \Lambda(y', x_\perp)) U_{y', \infty}(x_\perp). \quad (24)$$

Now we perform the integrations over Λ by expanding the path-ordered phases. It is most conveniently done by expanding the exponentials to first order on the rapidity grid with grid spacing a_y . This is a valid procedure as long as the function μ^2 is not divergent, $\lim_{a_y \rightarrow 0} a_y \mu^2(y) = 0$. We then perform all possible contractions with the propagator corresponding to the Gaussian weight in the path integral over Λ . Let us group together terms of the same order in the coupling constant. In zeroth order we have

$$\begin{aligned} & G_{ij;ab}^0(y, x_\perp; y', x'_\perp) \\ & = g^4 \delta_{ab} \int_{\max(y, y')}^\infty dy \mu^2(y, Q^2) \nabla_i \nabla_j \frac{1}{\nabla^4} (x_\perp, x'_\perp). \end{aligned} \quad (25)$$

Some comments are in order concerning the inversion of the operator ∇^4 , since there is an infrared singularity in the inversion. Recall that the sources of interest ultimately arise from individual nucleons. Therefore all effects of sources die off at transverse size scales larger than $1/\Lambda_{\text{QCD}}$. The charge itself averaged over such transverse size scales also vanishes. This means that the Green's function should be defined with boundary conditions that ensure its vanishing at distance $1/\Lambda_{\text{QCD}}$. In other words, whenever an infrared cutoff is needed for a proper definition of an inverse of a differential operator, it should be taken of the order of $1/\Lambda_{\text{QCD}}$. We will see that the quantities of physical interest are only very weakly dependent on this nonperturbative length scale, but nevertheless such a dependence does not disappear entirely.

Here and in all that follows, we will define

$$\gamma(x) := \frac{1}{\nabla^4} (x) = \frac{1}{8\pi} x^2 \ln(x^2 \Lambda_{\text{QCD}}^2) + \gamma(0), \quad (26)$$

where $\gamma(0)$ denotes an (infrared-divergent) constant which ensures the vanishing of this Green's function as x_\perp approaches the infrared cutoff $1/\Lambda_{\text{QCD}}$. Fortunately, the correlation function we will calculate below does not depend on the value of $\gamma(0)$ and the only infrared sensitivity that remains is through the logarithmic term in Eq. (26).

In first order, a quick computation gives

$$G_{ij}^1(y, x_\perp; y', x'_\perp) = -\frac{1}{2} \delta_{ab}(-N_c) \times \left[g^4 \int_{\max_{y, y'}}^{\infty} dy'' \mu^2(y'', Q^2) \right]^2 \times [\nabla_i \nabla_j' \gamma(x_\perp - x'_\perp)] [\gamma(x_\perp - x'_\perp) - \gamma(0)]. \quad (27)$$

In this equation, N_c is the number of colors.

Similarly, in n th order, we find

$$G_{ij,ab}^n(y, x_\perp; y', x'_\perp) = (-1)^n \delta_{ab} \frac{(-N_c)^n}{(n+1)!} \left[g^4 \int_{\max_{y, y'}}^{\infty} dy'' \mu^2(y'', Q^2) \right]^{(n+1)} \times \nabla_i \nabla_j' \gamma(x_\perp - x'_\perp) \{ \gamma(x_\perp - x'_\perp) - \gamma(0) \}^n. \quad (28)$$

The tadpole terms which take care of subtractions of $\gamma(0)$ appear through the normal ordering of the path-ordered exponential. This calculation can be found in Appendix A.

We can now sum the series and find a representation for the correlation function as (assuming $y > y'$)

$$G_{ij}^{ab}(y, x_\perp; y', x'_\perp) = -\delta^{ab} (\nabla_i \nabla_j' \gamma(x_\perp - x'_\perp)) \times \frac{1}{N_c [\gamma(x_\perp - x'_\perp) - \gamma(0)]} \times (1 - \exp\{g^4 N_c \chi(y, Q^2)\}) \times [\gamma(x_\perp - x'_\perp) - \gamma(0)], \quad (29)$$

where we have defined

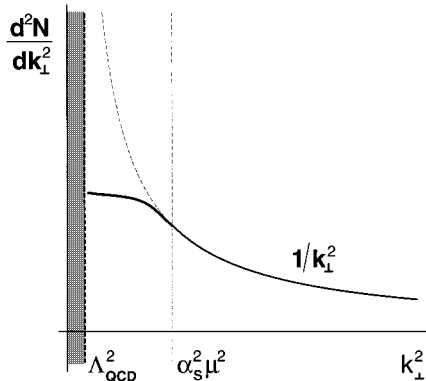


FIG. 1. Distribution at fixed x as a function of intrinsic transverse momentum k_\perp^2 . We obtain considerable softening at small k_\perp^2 compared to the perturbative $1/k_\perp^2$ behavior.

$$\chi(y, Q^2) = \int_y^\infty dy' \mu^2(y', Q^2). \quad (30)$$

The quantity $\chi(y, Q^2)$ is the total charge squared per unit area at rapidity greater than the rapidity y .

Finally, for the distribution function we get

$$G_{ii}^{aa} = \frac{4(N_c^2 - 1)}{N_c x^2} [1 - (x^2 \Lambda_{\text{QCD}}^2)^{(q^4 N_c / 8\pi) \chi(y) x^2}]. \quad (31)$$

This correlation function has an amusing structure. At small transverse distances where γ approaches zero, the correlation function tends to the perturbative correlation function, that is, its value in lowest order in an expansion in g^2 . At short distances, the theory is perturbative. At large transverse distances (but of course still much smaller than $1/\Lambda_{\text{QCD}}$), the correlation function dies off like $1/x^2$. Its Fourier transform at small momenta therefore behaves as

$$G(y, y' = y, k_\perp) \sim \ln[k_\perp^2 / g^4 N_c \chi(y)]. \quad (32)$$

This is in contrast to the behavior at larger transverse momentum where this correlation functions rises like $1/k_\perp^2$ as k_\perp decreases, in agreement with the perturbative result. The correlation function is therefore much softened at small k_\perp . This behavior is shown in Fig. 1. The characteristic momentum scale which differentiates between the nonperturbative and perturbative regions is $k_\perp^2 \sim g^4 N_c \chi(y)$, that is, g^4 times the charge per unit area at rapidities greater than the rapidity at which the correlation function is measured.³ This nonperturbative regime is nevertheless a weak coupling regime. Only when $k_\perp^2 \sim \Lambda_{\text{QCD}}^2$ does the coupling become strong and weak coupling methods can no longer be used.

It is worth noting that the dependence upon Λ_{QCD} is very weak. At large transverse momenta the Fourier transform of the distribution function G does not depend on Λ_{QCD} . At large separations there is saturation, and there is again no dependence upon Λ_{QCD} . The dependence is really only in the region of very small momenta ($k_\perp \ll \alpha_s \chi$), where our approximation is in any case not valid.

This result is almost consistent with the structure which was argued to be true by McLerran and Venugopalan [2]. They had argued that at small transverse momentum the above correlation function should approach a constant. It does up to logarithmic corrections. (The line of reasoning in Ref. [2] was, however, incorrect since it was based on an analysis of an equation that did not properly handle the induced charge associated with the gluon field, that is, the $[A_i, \partial^+ A^i]$ term in the equation which determines the gluon field in terms of the external charge density.)

³As we will see in the next section, the contribution of the gluons to χ is proportional to N_c at large N_c . In the large- N_c limit, the coupling constant scales as $g^2 N_c = \text{const}$. The crossover scale therefore has the correct large- N_c scaling behavior.

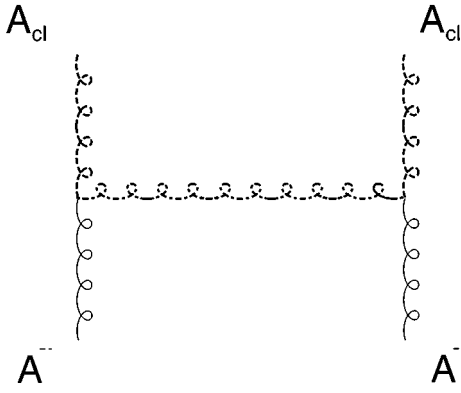


FIG. 2. Leading perturbative correction to the gluon distribution beyond the classical field approximation. The thick lines denote gluons with large longitudinal momentum p^+ . The momentum of the thin lines is k^+ . The large logarithms come from the kinematical region $k^+/p^+ \ll 1$.

III. RENORMALIZATION-GROUP-IMPROVED CHARGE DISTRIBUTION AND GLUON FIELD

In previous work, it was shown that radiative corrections to the distribution functions computed in the McLerran-Venugopalan model are large [7]. The first order correction comes from the diagram of Fig. 2.

The modification of the distribution function is of order $\alpha_s \ln(1/x) \ln(k_\perp/\alpha_s \mu)$ at large k_\perp and small x . For $k_\perp \sim \alpha_s \mu$, the natural k_\perp scale in the problem, the corrections are of order $\alpha_s \ln(1/x)$. In any case, for small values of x , these corrections become large and cannot be ignored.

In this section, we will set up a renormalization group procedure that sums up these corrections. The method of analysis is the following. We first consider the bare McLerran-Venugopalan model with a fixed valence charge density and a fixed ultraviolet cutoff in the longitudinal momentum P^+ . Physically, P^+ is of the order of the longitudinal momentum of the nucleus. It sets the scale of size for the longitudinal extent of the nucleus.

The renormalization group is implemented by considering the effective Lagrangian at a scale of momentum k^+ much less than P^+ , but where $\alpha_s \ln(1/x) \ll 1$. To generate this effective Lagrangian, we integrate out quantum fluctuations with momentum $k^+ \leq q^+ \leq P^+$. This procedure, as will be seen, generates a new effective Lagrangian of the same form as the original one, but with an additional charge squared per unit area. The typical scale of fluctuation of this additional charge squared per unit area is $\mu^2(y, Q^2) dy$ where $dy = -\ln(x)$ and Q^2 is a typical transverse momentum resolution scale at which the gluon distribution is ultimately measured.

Since the form of the Lagrangian is unchanged under integration of these high momentum modes, except for the overall scale factor μ^2 , the procedure can then be repeated and yet lower momentum modes can be integrated out. Importantly, as long as the coupling constant is small and also $\alpha_s \ln(x_1/x_2)$ is small, the quantum fluctuations can be integrated out perturbatively, so that the computation is controlled. This perturbative treatment considers fluctuations around the classical solution, in the region of the phase space which is being integrated out, as small. It is important to realize, however, that the classical solution itself in this re-

gion of momenta is changed relative to the one at the previous step of the RG procedure. This is because it solves classical equations in the presence of the additional charge $\mu^2(y, Q^2) dy$. This allows us to generate an effective Lagrangian at some scale of $x \ll 1$. This is in a region where the naive McLerran-Venugopalan model would have broken down.

Analogously, we can also allow the transverse momentum cutoff Q^2 to be changed independently by a renormalization group transformation. This corresponds to perturbatively integrating out quantum modes in a phase space region with transverse momenta between Q_1 and Q_2 . This latter RG transformation is the counterpart in our approach of the standard perturbative renormalization group scaling.

In the process of doing these transformations, we develop a set of renormalization group equations for $\mu^2(y, Q^2)$. These equations determine the rapidity and Q^2 dependence of this parameter.

We also determine the equation for the gluon field. It will turn out that this equation is a little more complicated than that in the previous section, since the induced charge depends upon the gluon field strength squared at the previous step of the renormalization group analysis. We argue that it should be a reasonable approximation to replace this field strength squared by its average value, in which case the equations described in the previous section can be derived. There are corrections to this approximation which are in principle computable. It is precisely this approximation which makes the fluctuations in the charge density uncorrelated in space-time rapidity. Inclusion of these corrections will induce correlations. These correlations will, however, on the average not contribute to building up the charge density.

It should be noted that there are other sources of correlation in longitudinal phase space. These arise from the classical field itself which is recomputed at each stage of the renormalization group analysis. Although it is true that the source of the color field is largely uncorrelated, for a given source, there are still long range correlations built into the color field which would yield nontrivial multiplicity correlations in rapidity.

Since the process closes under iteration, it is sufficient for us to show how we integrate the degrees of freedom as the Lagrangian changes scales in the N th to the $(N+1)$ st step of the renormalization grouping. This is what will be demonstrated below.

We begin our analysis with the McLerran-Venugopalan action

$$S = i \int d^2 x_\perp \frac{1}{\chi} \text{Tr} \rho^2(x_\perp) - \frac{1}{g^2} \int d^4 x \frac{1}{4} F_{\mu\nu} F^{\mu\nu} + \int d^4 x A^- J^+, \quad (33)$$

where

$$J^+(x) = \delta(x^-) \rho(x_\perp). \quad (34)$$

We are of course working in the $A^+ = 0$ gauge.

Now suppose we have a solution to the classical equations of the form

$$A^+ = A^- = 0,$$

$$A^i = \theta(x^-) \alpha^i(x_\perp). \quad (35)$$

It is understood in the above expressions that the longitudinal δ function (as well as θ function) is regularized on the scale $1/P_N^+$. Here P_N^+ is the typical longitudinal momentum of the fluctuations which have been integrated out in the previous step of the RG. At the very first step, of course, P^+ is the typical momentum associated with the nucleus or hadron. Clearly, knowledge of the precise structure of the charge density on the scales of order $1/P_N^+$ is necessary to determine the behavior of the classical solution at these scales.

However, in the following we will only need to know the structure of the solution at longitudinal momenta much smaller than P_N^+ . This is so even though we will integrate over the fluctuations in the entire momentum range

$$P_{N+1}^+ < k^+ < P_N^+, \quad (36)$$

where $P_{N+1}^+ \ll P_N^+$, but is still large enough so that $\alpha_s \ln(P_N^+/P_{N+1}^+) \ll 1$ (here α_s is evaluated at the scale χ and χ is assumed to be $\chi \gg \Lambda_{\text{QCD}}$). The reason is that the dependence on the upper cutoff is only logarithmic and the bulk of the contribution comes from much smaller momenta. To leading order, therefore, the results do not depend on the precise behavior of the classical field at the upper cutoff scale. Such is the magic of the logarithm, which enamored so many field theory practitioners. At momenta far below the cutoff, the classical field does not indeed have the structure $A^i(k) \propto 1/k^+ \alpha^i(k_\perp)$, which is equivalent to Eq. (35).

To compute the effective action, we must integrate out the fluctuations around the classical solution. As long as we only generate an effective action at a scale k^+ , so that $\alpha_s \ln(P_{N+1}^+/k^+) \ll 1$, then these fluctuations are small. We therefore have three types of fields to consider. There is the classical background field, the small fluctuation field at the scale of interest, and the fields at lower momentum scale. We need only keep terms in the action which are at most quadratic in the small fluctuation field. We will denote these fields in the following manner.

The field A_{cl}^N will be the classical background field. The label N refers to the N th step in the renormalization group procedure. This classical background field will be modified as the renormalization group procedure iterates. We will also write

$$A_{\text{cl}}^N = \theta_N(x^-) \alpha^N(x_\perp). \quad (37)$$

In this equation, as mentioned before, the step function is a step function on a distance scale larger than that which we have previously integrated out.

There are the small fluctuations fields at the step N which are within the momentum range that we integrate out. We will refer to these fields as δA^N .

Finally, there are the fields which are fluctuations around the classical solution at momentum scales much less than that where we perform the integration. These fields are not small. They are denoted as A^N .

The contribution to the effective action associated with the small fluctuation field is

$$\delta S = \frac{1}{g^2} \int d^2 x_\perp dx^+ \left\{ \int \frac{dk^+ dp^+}{4\pi^2} \left[\frac{1}{2} \delta A^N(k^+) D_N^{-1}(k^+, p^+) \delta A^N(p^+) \right. \right.$$

$$\left. \left. + 2 f_{abc} \int \frac{dk^+}{2\pi} \int_{-P_N^+}^{P_N^+} \frac{dk^{+'}}{2\pi} \alpha_a^{iN}(x_\perp) A_c^{-N}(k^{+'}, x^+, x_\perp) \delta A_{ib}^N(k^+, x^+, x_\perp) \right] \right\}. \quad (38)$$

In this equation, the momenta k^+ and p^+ are in the range between the cutoffs, $P_N^+ \leq |k^+|$, $|p^+| \leq P_{N-1}^+$. The momentum $k^{+'}$ is typically much softer than the lower cutoff and, therefore, also much softer than k^+ . The quantity D_N^{-1} is the inverse propagator in the background field. It depends on both the fields A_{cl}^N and A^N .

We have approximated the linear term in the small fluctuation by keeping only the eikonal part of the interaction vertex, that is, the coupling between the transverse components of the hard field and the minus component of the soft field. This will generate an effective action with only $+$ components of currents affected by integrating out the high momentum modes. The terms we neglected are suppressed by factors $k^{+'}/k^+$ and are subleading in the small- x region.

It is also understood that the transverse momenta of all the fields in Eq. (38) are bounded from above by some transverse cutoff Q . This is consistent with both the BFKL approach, where all transverse momenta are roughly the same, and the leading logarithmic (or double logarithmic at small

x) Altarelli-Parisi evolution, where the momenta are bounded by the momentum of the external probe. By imposing such a cutoff, we restrict ourselves to transverse momenta which are not parametrically large. This point can be appreciated by examining the Feynman diagrams. Consider, for example, the diagram that gives the leading correction to the distribution function beyond the classical field approximation. It is depicted in Fig. 2. The corrections of this type with arbitrary number of insertions of the background field have been calculated in Ref. [7]. For our present purposes, it is enough to consider the classical field expanded to first order in the charge density ρ . The diagram then is precisely the same as that of the standard perturbation theory. After the integration over the frequency k^- is performed, the correction to the distribution function is proportional to

$$\frac{1}{k^+ k_\perp^2} \int \frac{d^2 p_\perp}{p_\perp^2} \int_{k_N^+}^{k_{N-1}^+} dp^+ \frac{p^+}{[p^+ + k^+ (p_\perp^2 - 2p_\perp k_\perp)/k_\perp^2]^2}. \quad (39)$$

The transverse momentum integration in this expression is cutoff not at the scale k_{\perp}^2 (which is of the order Q^2), but rather k_{\perp}^2/x , which at small x is a very large scale. Physically, the part of the integration region above k_{\perp}^2 corresponds to emission of jets which are much harder than the probe. Precisely the same problem is encountered in the standard perturbative treatment [11]. These processes have to be considered separately, and at this point we will disregard them.

Equation (38) looks very suggestive. Introducing the notation

$$\delta\rho^a(x) = 2f_{abc}\alpha_b^{iN}(x)\delta A_{ic}^N(x), \quad (40)$$

we see that the linear coupling term between the soft field and the hard fluctuation is of the form

$$2\text{Tr}\delta\rho(x)A^-(x)\delta(x^-). \quad (41)$$

We would therefore like to integrate in the path integral over those components of the fluctuation field δA , which are ‘‘orthogonal’’ to $\delta\rho$. In other words, we would like to change variables from δA_{ib} to $\delta\rho^a$ and some X^a , and integrate over X . In fact, to get the result to the leading logarithmic accuracy it is not necessary to do it explicitly. Since $\delta\rho$ is linear in the fluctuation field and the integral over the fluctuation is Gaussian, it is clear that the result of the procedure described above will be of the form

$$\begin{aligned} & \int [d\delta A] \exp\{i\delta S\} \\ &= M(\alpha) \int [d\delta\rho] \exp\left\{-\int_{x,y} \frac{1}{2}\delta\rho^a(x)\delta\rho^b(y)\right. \\ & \quad \left.\times [\delta\chi]_{ab}^{-1}(x,y) + i\delta\rho^a(x)A_a^{-N}(x)\right\}. \end{aligned} \quad (42)$$

Here M is the contribution of the determinant which arises in the Gaussian integration over X . To the leading logarithmic accuracy, this contribution can be ignored. This amounts to neglecting the loop corrections with all particles in the loop having the longitudinal momentum in the same range $P_N^+ \leq p^+ \leq P_{N-1}^+$. Corrections of this type do not give large contributions at small x [11]. It was also shown in the previous analysis [7] that such contribution could be ignored at small x for modifications to the Weizsäcker-Williams background field.

The matrix $\delta\chi_{ab}(x,y)$ is given by

$$\begin{aligned} \delta\chi_{ab}(x,y) &= 4i \int_{P_N^+ \leq |p^+| \leq P_{N-1}^+} \frac{dp^+}{2\pi} f^{acd}f^{bef}\alpha_i^c(x_{\perp})\alpha_j^e(y_{\perp}) \\ & \quad \times D_{ij}^{Ndf}(p^+, x_{\perp}, x^+, y_{\perp}, y^+). \end{aligned} \quad (43)$$

To proceed further, we need to know the structure of the propagator of the hard fluctuations D^N . Since the longitudinal momentum scale in the propagator is large, we can use a no recoil or eikonal approximation to incorporate the effect of interaction with the softer fields A^{N-} . The calculation is given in Appendix B.

In the eikonal limit, the propagator is

$$\begin{aligned} & D_{ij}^{Nab}(K^+, z^-; x^+, x_{\perp}, y^+, y_{\perp}) \\ &= \delta_{ij}\delta(x_{\perp}-y_{\perp}) \frac{\text{sgn}K^+}{K^+} i\theta(K^+(x^+-y^+))\hat{P} \\ & \quad \times \exp\left[-i\int_{y^+}^{x^+} dz^+ \mathbf{A}_{\text{adj}}^-(\mathbf{z}^+, \mathbf{z}^-, \mathbf{x}_{\perp})\right]^{ab}. \end{aligned} \quad (44)$$

In this equation, $\mathbf{A}_{\text{adj}}^-$ and, hence, the path-ordered phase are in the adjoint representation. In the phase, the dependence upon x^- can be ignored since the function is slowly varying on scales of the typical size corresponding to $1/k^+$. Here we have taken K^+ as the momentum conjugate to the difference of coordinates $x^- - y^-$, and $z^- = (x^- + y^-)/2 \sim x^- \sim y^-$ is the average position associated with the field.

The expression above accounts only for soft fields with longitudinal momenta smaller than that of the fluctuation δA . In terms of Feynman diagrams, this corresponds to summation of the diagrams of the type depicted on Fig. 3. In fact, the propagator D^N also depends on the background field $\alpha_i^a(x_{\perp})$ and this dependence is important in parts of the phase space. These contributions are of the type Fig. 4. We will come back to this point and discuss the importance of these terms later. Temporarily, however, we will disregard them in order to make the discussion conceptually simpler.

As for the soft insertions, the following remark is in order. The propagator depends only on the minus component of the vector potential. On the classical solution discussed in the previous section, this component vanishes. It is therefore only the fluctuations of A^- around the new classical solution that contribute to D . Since these effects are higher order in the coupling constant, we will ignore them to this order. Again, these corrections too are important at low transverse momentum. This point will be addressed in Sec. V.

With these approximations the fluctuation propagator becomes very simple. The fluctuation of the charge density $\delta\mu^2$ is time (x^+) independent and local in the transverse directions:

$$\begin{aligned} \delta\chi_{ab}(x_{\perp}, y_{\perp}) &= \frac{1}{g^2\pi} dy_N \delta^2(x_{\perp}-y_{\perp}) f^{acd}f^{bed} \\ & \quad \times \alpha_i^c(x_{\perp})\alpha_i^e(x_{\perp}). \end{aligned} \quad (45)$$

Note that since our fields have a built in cutoff on the transverse momentum, the $\alpha(x_{\perp})\alpha(x_{\perp})$ actually should be understood as averaged on a transverse scale size $d^2x_{\perp} \sim 1/Q^2$.

We now make the approximation

$$\alpha_i^a(x_{\perp})\alpha_j^b(x_{\perp}) \approx \langle \alpha_i^a(x_{\perp})\alpha_j^b(x_{\perp}) \rangle = \frac{1}{2(N_c^2-1)} \delta^{ab}\delta_{ij}\langle \alpha^2 \rangle. \quad (46)$$

The averaging in Eq. (46) is over the distribution of ρ . We believe this approximation should be adequate to describe the RG flow of χ , especially at large Q . The fluctuations of ρ are very short range in the transverse direction. On the other hand, the fields α are slowly varying, its transverse correlation length being of order $1/g^2\chi$. There is therefore very little

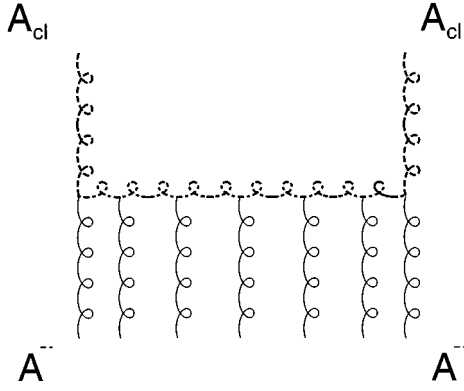


FIG. 3. Same as in Fig. 2, but with additional insertions of the soft external field. These diagrams give corrections to the distribution function upon contracting the soft legs. They therefore correspond to the virtual corrections and are higher order in fluctuation fields.

correlation between $\rho(x_\perp)$ and the field $\alpha(x_\perp)$ at the same point. Also, because of slow variation of $\alpha(x_\perp)$ in space, an approximation of $\alpha^2(x_\perp)$ by an x_\perp -independent constant should be good with accuracy $g^2\chi/Q$. Although this approximation is true on the average, it ignores some of the correlations which are built into the longitudinal structure. It would be very important to study corrections to this approximation or better yet to fully incorporate the structure of Eq. (45) in the solution to the problem. This is left for further study.

We get, therefore, that the change in the charge density is governed by the parameter

$$\delta\chi_N(Q^2) = \frac{1}{g^2\pi} \frac{N_c}{(N_c^2-1)} dy_N \langle \alpha_N^2 \rangle_{Q^2}. \quad (47)$$

The variation of χ due to the change of the transverse cutoff is also easily calculated:

$$\delta\chi_N(Q^2) = dQ^2 \frac{N_c}{(N_c^2-1)} \frac{1}{g^2\pi} \sum_{P=1}^N dy_P \langle \alpha_P(Q)^2 \rangle. \quad (48)$$

The change in the effective action is, therefore,

$$\begin{aligned} & \exp\{i\delta S\} \\ &= \int [d\delta\rho_N] \exp\left(-\int d^2x_\perp \frac{1}{\delta\chi_N(Q^2)} \text{Tr}\delta\rho_N^2(y, x_\perp)\right) \\ & \times \exp\left(i \int d^2x_\perp \int_{-\infty}^{\infty} dx^+ \delta\rho_N(x_\perp) A_N^-(x_\perp, x^+)\right). \quad (49) \end{aligned}$$

Now we identify some typical space-time rapidity for our source with the momentum space rapidity. We expect that $y_{\text{space-time}} \sim y_{\text{mom}}$. Let us define

$$y = y_0 - \sum_{i=1}^N dy_i, \quad (50)$$

where the the right-hand side is the momentum space rapidity shifts induced by integrating out the different scales. We will see that the left-hand side has an interpretation of the

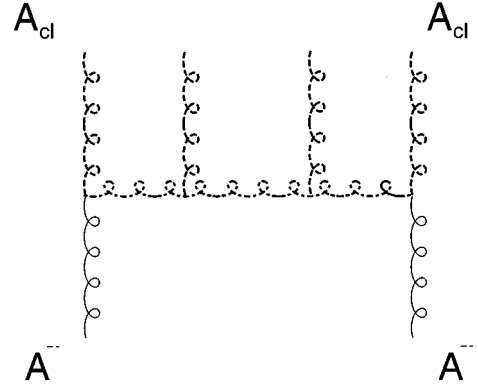


FIG. 4. Same as in Fig. 2, but with additional insertions of the hard background field. These diagrams are important in the region of momenta Q of order $\alpha_s\chi$. See the discussion in the next section.

space-time rapidity. The rapidity y_0 is the beam rapidity. We see that the equation for the evolution of χ generated by our renormalization group procedure can be written as [12,13]

$$d\chi(y, Q^2)/dy dQ^2 = \frac{N_c}{N_c^2-1} \frac{1}{(2\pi)^2} \frac{1}{g^2\pi} \langle \alpha(y, Q)^2 \rangle. \quad (51)$$

This equation can be either formulated as a BFKL-type equation, when one does the integral of Q first, or as a DGLAP-type equation, if one does the integral over y first [14]. Notice that it is a nonlinear generalization of both equations, since the right-hand side of the equation is a function of χ .

This equation has a simple physical interpretation. The factor of $N_c/(N_c^2-1)$ is the charge squared per gluon. The number of gluons contained in our classical field is

$$dN/dy dQ^2 = \frac{1}{(2\pi)^2} \frac{1}{g^2\pi} \alpha(y, Q)^2. \quad (52)$$

What our analysis has shown is that the change in charge squared is entirely due to the change in the number of gluons due to new phase space opening up. Of course, this is a nonlinear problem in general since the source of charge changes the classical background field in a nontrivial way.

Let us also define

$$\rho(y, x_\perp) = \delta\rho_N(x_\perp)/dy \quad (53)$$

and

$$A_N^-(x_\perp, x^+) = A^-(x_\perp, x^+, y). \quad (54)$$

Now we must compute the change in the classical field. Since the change in the classical field is small, we see that if we write

$$A_{N+1}^{\text{cl}} = \delta A_N^{\text{cl}} + A_N^{\text{cl}}, \quad (55)$$

we can linearize the equations for δA_N^{cl} . We find that $\delta A_{N+1, \text{cl}}^- = 0$ and that

$$D^i(A_N^{\text{cl}}) \partial^+ \delta A_{Ni}^{\text{cl}} + [\delta A_N^{\text{cl}}, \partial^+ A_N^{\text{cl}}] = g^2 \delta_N(x^-) \delta\rho_N/dy. \quad (56)$$

In this equation, $\delta_N(x^-)$ means a delta function on the scale of our new classical field; that is, as a regularized distribution it has its support on the scale $1/P_N^+$. Now we define δA_N^{cl} to vanish on the scale of the old classical field. Therefore only the first term survives.

Upon identifying the index N with the space-time rapidity, we see that our classical equation solves the equation we posited in the last section that

$$D_i(A^{\text{cl}}) \frac{d}{dy} A^i = g^2 \rho(y, x_\perp). \quad (57)$$

(The easiest way to see this is to break up space-time rapidity into discrete intervals. Identify an index with each interval. Precisely the renormalization group equation for the field results.)

We also see that the path integral measure for the fluctuating field is what we postulated in the previous section, with one caveat: We have omitted some contributions which on the average vanish in their contribution to the induced χ . These terms generate a nontrivial correlation in rapidity beyond which we compute. We will not further discuss their inclusion here except to note that they in principle are computable and should be included at some point.

IV. RG EQUATIONS FOR $\chi(y, Q^2)$

We now discuss the renormalization group equation (51). This equation determines how the color charge per unit area scales with rapidity and a transverse resolution scale size Q^2 .

The consistency of our analysis requires that the solution to the renormalization group equation only involve information in the region where our approximate methods of computation are valid. It could easily happen that the region of interest in transverse space after several steps in the renormalization group procedure might drift to some value where our approximations are no longer valid. This might happen if at some rapidity y the relevant typical values of Q^2 became of order Λ_{QCD}^2 or became much greater than $\mu^2(y, Q^2)$ where our classical source size approximation breaks down. It is plausible that the region of integration for the solution of the equations involves primarily the region of interest, since this is physically where the field originates, but we have no proof. In addition, the region of large Q^2 where our classical methods no longer apply is probably correctly treated even though the derivation above breaks down. In this region, the fields are weakly coupled, and our expression derived by classical means appears to be correct even in this region, to leading order in coupling.

The renormalization group equation may be formulated in the DGLAP form by first integrating over y as

$$d\chi/dQ^2 = \frac{N_c}{(N_c^2 - 1)} \frac{1}{(2\pi)^2} \frac{1}{g^2 \pi} \int_y^{y_b} dy' \langle \alpha(y', Q^2)^2 \rangle. \quad (58)$$

It may be written in the BFKL-like form as

$$d\chi/dy = \frac{N_c}{(N_c^2 - 1)} \frac{1}{(2\pi)^2} \frac{1}{g^2 \pi} \int_0^{Q^2} dQ'^2 \langle \alpha(y, Q'^2)^2 \rangle. \quad (59)$$

Note that this is a nonlinear equation. The dependence of its right-hand side on χ is determined by the solution of classical equations.

At this point we want to return to a discussion of the terms that we have neglected in deriving Eq. (51), namely, the contributions of the diagrams of Fig. 4, with insertions of a hard background field. From the perturbative point of view, those correspond to modifications of the gluon distribution due to mixing between the two-particle and multiparticle (higher twist) operators. These diagrams can in principle be taken into account by using instead of the free propagator in Eq. (43) the full propagator in the external field as calculated in [7].

Although this calculation has yet to be performed, it is easy to understand qualitatively the main modifications it will bring about. First, even with the inclusion of the background field the additional charge density $\delta\rho$ will remain static. This is due to the fact that all the internal lines in the diagram Fig. 4 have the frequency (p^-) of the order of the on-shell frequency corresponding to the longitudinal momentum $P_N^+ \leq p^- \leq P_{N-1}^+$. It is much smaller than the on-shell frequency of the external line with momentum k^+ . From the point of view of the emitted particle, therefore, the coupling is always to the static source. The main effect of these extra insertions will be to modify the right-hand side of Eq. (51) by adding to it terms nonlinear in $(\alpha)^2$. This effect, however, will be significant only for Q of order $g^2\chi$. Physically, the diagrams of Fig. 4 describe an emission of the soft particle with transverse momentum k_\perp by a classical field $\alpha_i(x)$. Clearly, as long as the transverse momentum of the emitted particle is larger than the inverse correlation length of the field, the particle is emitted locally. In this case the emission probability depends only on $\alpha^2(x)$ at the point of emission. In the local limit, therefore, the effect of these corrections will be of order $\alpha^2(x)/k_\perp^2$. At large Q the main contribution to the distribution function comes from large k_\perp^2 , and the correction due to nonlinearities is therefore negligible. At Q of order $g^2\chi$ and smaller, the contribution of the diagrams in question is important. However, in the saturation regime $Q \leq g^2\chi$ they do not change the behavior qualitatively. In this region there is practically no running of χ with y . The reason is that since the correlation length of the classical field is of order $(g^2\chi)^{-1}$, the phase space for emission shrinks to zero at these values of momenta.

The qualitative features of the solution of our RG equation are these. In the region of large Q^2 , the equation approximately linearizes to become

$$d^2\chi/dy d \ln Q^2 = \frac{N_c \alpha_s}{\pi} \chi. \quad (60)$$

This is precisely the double-logarithmic approximation to the DGLAP equation [14]. It would be solvable if it were not for the dependence of α on χ . If we hold this fixed, we get approximately (assuming that χ is a slowly varying function of y at some Q_0^2) that

$$\chi = \exp \left\{ 2 \sqrt{\frac{N_c \alpha_s}{\pi}} y \ln Q^2 / Q_0^2 \right\}. \quad (61)$$

The dependence of α_s upon χ will of course modify the solution.

In the region of transverse momenta in the vicinity of the crossover scale $\alpha_s \chi$, the nonlinearities in the renormalization group equation become important. It is likely that one of the effects of this will be that the transverse phase space in this region will be a very slowly varying function of Q^2 . It is then more convenient to turn to the form (59). Assuming this to be the main effect of the nonlinearities and approximating the transverse phase space by a constant P , we can write the solution as

$$\chi = \chi_0 \exp\left\{\frac{N_c \alpha_s}{\pi} P y\right\}. \quad (62)$$

This has the BFKL-type behavior, growing as a power at small x . To calculate the value of the constant P , we would have to include virtual corrections which have been neglected so far.

Finally, in the saturation region where $Q^2 \ll \alpha_s^2 \chi(y, Q^2)$, the right-hand side is constant up to logarithms. Here the solution is, to a good approximation,

$$\chi = \chi_0 + \kappa(y_0 - y)Q^2, \quad (63)$$

where κ is some slowly varying function. There is little change until $(y_0 - y)Q^2/\chi_0$ becomes of order 1.

V. UNITARITY, TOTAL MULTIPLICITY, AND SUMMARY

The issue of unitarity in deep inelastic scattering is related to the x dependence of

$$G(x, Q^2) = \int_0^{Q^2} d^2 p_\perp \frac{dN}{dx d^2 p_\perp}, \quad (64)$$

at fixed Q^2 as x decreases. We have seen that at fixed p_\perp there are two separate regions for $dN/dx d^2 p_\perp$. The first is at large $p_\perp^2 \gg \alpha_s^2 \chi(x)$. In this region, the integral above is $xG(x, Q^2) \sim \ln(Q^2) \chi(x)$ up to factors of logarithms of μ . As x decreases, this is a rapidly rising function of $1/x$.

At some point, for any fixed Q^2 , the parameter χ will become $\leq Q^2$. At this point, we are in the small- p_\perp region for the computation of $dN/dx d^2 p_\perp$. In this region, $dN/dx d^2 p_\perp \sim \ln(p_\perp)$ up to factors of $\ln(\chi)$. (It would be useful to determine these factors more accurately and actually compute the cross section in this region, but again this is beyond the scope of this paper.) Here the structure function xG has at most a logarithmic dependence upon x . There is therefore no obvious contradiction with unitarity. The dependence of xG on Q^2 is also amusing, rising like some power of Q^2 up to logarithms, until saturating at χ .

The total multiplicity produced in hadron-hadron collisions at x may also be estimated. Here we return to rapidity variables. On scaling grounds alone, the multiplicity of produced gluons per unit area should be $dN_g/dy \pi R^2 \sim \chi(y, \eta \sim 1)$. These gluons after production interact at high relative energy and, therefore, largely elastically. The number of gluons should be approximately conserved. Later, as a quark-gluon plasma is formed, the system

expands approximately isentropically, so that the total number of gluons produced should be roughly the same as the number of pions.

At this point, we do not have a full solution of the renormalization group equation in hand. Suffice it to say that one expects a rapid growth of the parameter χ as x decreases at large p_\perp . This should be much faster than a power of a logarithm of beam energy. The reason that this growth does not violate unitarity is because it is arising from an enhanced contribution at larger transverse momenta.

The typical transverse momentum in this picture will go as the square of the multiplicity per unit area. The total deposited energy density at a typical formation time $t \sim 1/\chi$ will be of order χ^4 . All of these functions are expected to be asymptotically somewhat rapidly rising functions of energy.

To summarize, the results of this work are extremely suggestive. We have presented a picture of low- x gluon structure functions which has many of the intuitive features normally associated with the Pomeron. The calculation presented here should be improved, however, in many aspects.

We have made several drastic approximations in deriving the renormalization group equation. Let us once again point those out.

First, we have neglected the virtual corrections. Those are generated by the diagrams in Fig. 3 when one contracts the external legs. Formally, as we mentioned in Sec. III, those are higher order in fluctuation and for that reason would seem to be subleading. However, some of these diagrams are known to contribute to the BFKL equation and, therefore, must be important at least in some kinematic regime. This suggests that the generic form of the effective action which we have relied on, Eq. (49), is not quite complete. To see what is missing, let us consider for a moment fields in three ranges of the longitudinal momentum: the field $A_\mu(k^+)$ with $k^+ \geq P_{N-1}^+$, the field $B_\mu(l^+)$ with $P_{N-1}^+ \geq l^+ \geq P_N^+$, and the field $C_\mu(m^+)$ with $m^+ \leq P_N^+$. The integration over A and B generates the effective action for C . Taking into account the soft insertions of Fig. 3 means we should use for the fluctuations propagator the full eikonal expression (45) without setting the Wilson line factor equal to unity. The integration over the fluctuations of the field A_μ will generate the effective Lagrangian

$$\begin{aligned} & i \int d^2 x_\perp \text{Tr} \delta \rho_{N-1}(x_\perp) \frac{1}{\bar{\chi}_{N-1}(B^- + C^-)} \delta \rho_{N-1}(x_\perp) \\ & + \int d^2 x_\perp \int_{-\infty}^{\infty} dx^+ \delta \rho_{N-1}(x_\perp) [(B^-(x_\perp, x^+) \\ & + C^-(x_\perp, x^+)], \end{aligned} \quad (65)$$

where

$$\bar{\chi}_{N-1}(B^- + C^-) = \delta \chi_{N-1} W(B^- + C^-) \quad (66)$$

and

$$W(A^-) = \hat{\mathbf{P}} \exp \left[-i \int_{-\infty}^{\infty} dz^+ \mathbf{A}_{\text{adj}}^-(\mathbf{z}^+, \mathbf{x}_\perp, \mathbf{x}^- = \mathbf{0}) \right]. \quad (67)$$

In the next step the integration over the fluctuations of B leads to the effective Lagrangian for C :

$$\begin{aligned} & \int d^2x_{\perp} \int_{-\infty}^{\infty} dx^+ [\delta\rho_{N-1}(x_{\perp}) + \delta\rho_N(x_{\perp})] C^-(x_{\perp}, x^+) \\ & + i \int d^2x_{\perp} \text{Tr} \delta\rho_{N-1}(x_{\perp}) \frac{1}{\langle \bar{\chi}_{N-1}(B^- + C^-) \rangle_B} \\ & \times \delta\rho_{N-1}(x_{\perp}) + i \int d^2x_{\perp} \text{Tr} \delta\rho_N(x_{\perp}) \frac{1}{\bar{\chi}_N(C^-)} \delta\rho_N(x_{\perp}). \end{aligned} \quad (68)$$

In the second term the angular brackets denotes averaging over the fluctuation of the field B :

$$\begin{aligned} \langle \bar{\chi}_{N-1}(B^- + C^-) \rangle_B &= \delta\chi_{N-1} \int [d\delta B] W(B+C) \\ &= (1-\gamma) \delta\chi_{N-1} W(C). \end{aligned} \quad (69)$$

We see, therefore, that the integration over the fluctuations in the range of momenta between P_{N-1}^+ and P_N^+ not only generates the additional charge density $\delta\rho_N$, but also modifies the fluctuation amplitude of the charge density ρ which is generated by the higher momentum modes $k^+ \geq P_{N-1}^+$. This modification is only important for the coupling of the density ρ to the fields with momenta $m^+ \leq P_N^+$, since only in this case is the longitudinal phase space large and the correction factor γ proportional to $\ln(1/x)$. In terms of Feynman diagrams, this calculation corresponds to the virtual corrections of Fig. 5 and the factor γ is directly related to the so-called non-Sudakov form factor [11]. It is important to note that even though the form of effective Lagrangian (68) is not precisely the same as considered in Sec. II, on the classical solutions where $A^- = 0$ the two indeed coincide. This is so, since the Wilson loop operator depends only on one component of the gauge field A^- . Therefore, for $A^- = 0$, the charge density fluctuation $\bar{\chi}_N$ depends only on the charge density ρ_{N-1} and Eq. (68) reduces to Eq. (43). The solution considered in Sec. II is therefore still applicable to the modified Lagrangian. The net effect of the virtual corrections is to modify the running of the effective charge density $\chi(y)$ through the change on the right-hand side of the renormalization group equation (51). This effect is calculable and should indeed be calculated, but this is beyond the scope of this paper. We will only note that since these virtual diagrams do not play any role in the perturbative double-logarithmic DGLAP treatment and our renormalization group equation reduces to it in the limit of large Q , we expect these extra corrections to be important only in the non-linear regime $Q \sim \alpha_s \chi$.

The second approximation that we made was to neglect the insertions of the hard background field. This was discussed in the previous section, where we have argued that these corrections are also unimportant at large Q . Again, in principle, these corrections are calculable by using the full fluctuation propagator in the background field, as calculated in [7].

The third approximation in arriving at Eq. (51) was to replace the square of the classical field by its average. This led to the absence of correlations in rapidity for the density fluctuations. This approximation is also expected to be good

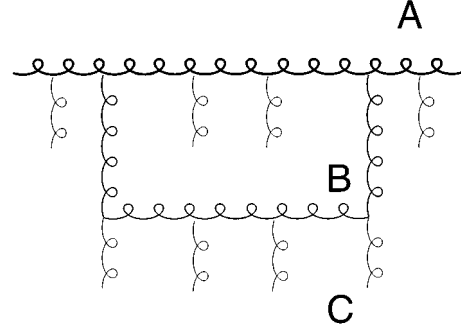


FIG. 5. Virtual corrections of Eq. (68). The thickest line denotes the propagator of the field component A with the largest longitudinal momentum. The thick line that completes the loop is the propagator of the field B . Finally, the thin external lines denote the external field C , for which the effective Lagrangian is being computed.

for large transverse momenta, where the emission of a soft field is local in transverse coordinates and therefore the additional density $\delta\rho$ is practically uncorrelated with the density coming from higher rapidities. At transverse momenta of order of the inverse correlation function of the classical field, this approximation should break down.

Clearly, the treatment of the nonlinear region $Q \leq \alpha_s \chi$ in the present paper is very rudimentary. It is in great need of improvement, and we intend to address this problem in future work. In fact, at small transverse momenta the very notion of the momentum cutoff Q is highly questionable. The density-density correlation which is given by the diagram in Fig. 2, in momentum space, is a very slowly varying function of the transverse momentum at $k_{\perp} \gg \alpha_s \chi$. It depends on the momentum logarithmically. In this range of momenta, one can therefore approximate it by a constant. In our calculation precisely this is achieved by introducing the cutoff Q and using the eikonal approximation for the propagator D_N , which results in a local correlator of density in the transverse coordinates. At momenta of order $\alpha_s \chi$, however, the correlator changes rapidly. Approximating it by a constant with some transverse cutoff should therefore result in an error of order 1. A more careful treatment will bring about nontrivial transverse correlations of the charge density. One should therefore expect that an improved treatment of the low transverse momenta region will modify the distribution for density fluctuations such that nontrivial transverse as well as longitudinal correlations will appear. The effective Lagrangian which would generate the classical solutions will be of the form

$$\begin{aligned} & \int dy dy' d^2x_{\perp} d^2x'_{\perp} \text{Tr} \rho(y, x_{\perp}) \\ & \times [\mu^2(y, y', x_{\perp}, x'_{\perp})]^{-1} \rho(y', x'_{\perp}). \end{aligned} \quad (70)$$

In fact, in a general case there is no reason to expect that the weight will be Gaussian, so that the weight function μ could itself depend on ρ .

It remains to be seen how large in fact will be the effect of these improvements. We believe that although quantitatively

it should be significant, the qualitative picture presented here will be confirmed. If the above issues can be answered in a satisfactory way, then one can proceed to a detailed computation of hadronic interactions within this approach. Deep inelastic scattering from nuclei and Drell-Yan production in heavy ion collisions might be computed. The initial conditions for nucleus-nucleus collisions might be found in detail. The fluctuation spectra and correlations between fluctuations would also do much to verify the above picture. It would be very useful to have data on the structure functions directly by using nuclei in the DESY ep collider HERA.

ACKNOWLEDGMENTS

We gratefully acknowledge the contributions of Rajiv Gvai and Raju Venugopalan whose careful work showed that the original treatment advocated by McLerran and Venugopalan led to infrared singular correlation functions. We thank Jianwei Qiu and Mark Strikman for interesting discussions and Al Mueller for informing us of the work of Yuri Kovchegov [9] which we received when this paper was being written. This work was supported by DOE Contracts Nos. DOE High Energy DE-AC02-83ER40105 and DOE-Nuclear DE-FG02-87ER-40328.

APPENDIX A: NORMAL ORDERING THE DISTRIBUTION FUNCTION

We have to calculate

$$G_{ij}(y, x_\perp; y', x'_\perp) = \int [d\rho] \exp\left(-\int dy'' d^2x''_\perp \frac{1}{2\mu^2(y'', Q^2)} \rho^2(y'', x''_\perp)\right) i^2 U(y, x_\perp) \nabla_i U^\dagger(y, x_\perp) U(y', x'_\perp) \nabla_j U^\dagger(y', x'_\perp). \quad (\text{A1})$$

This can be cast in the form

$$G_{ij}(y, x_\perp; y', x'_\perp) = \left\langle \int_y^\infty dy' \{U_{\infty, y'}[\nabla^i \Lambda(y')] U_{y', \infty}\}(x_\perp) \int_{y'}^\infty d\bar{y}' \{U_{\infty, \bar{y}'}[\nabla^i \Lambda(\bar{y}')] U_{\bar{y}', \infty}\}(\bar{x}_\perp) \right\rangle_\Lambda, \quad (\text{A2})$$

with the correlation function

$$\langle \Lambda(y, x_\perp) \Lambda(y', x'_\perp) \rangle_\Lambda = g^4 \mu^2(y, Q^2) \delta(y - y') \gamma(x_\perp - x'_\perp). \quad (\text{A3})$$

The function γ is given in Eq. (26) and, as discussed in Sec. II, is infrared singular. The leading dependence on the infrared cutoff resides in the constant term $\gamma(0)$. Fortunately, all terms containing $\gamma(0)$ cancel in the expression for the correlation function. To understand how these cancellations work in Eq. (A3), let us first consider the normal ordering of individual link operators first. To do so, let us break up any link operator from y to ∞ into ‘‘infinitesimal factors’’:

$$U_{\infty, y}(x_\perp) = \lim_{k \rightarrow \infty} \prod_{n=1}^k U_{\infty, y_k}(x_\perp) U_{y_k, y_{k-1}}(x_\perp) \times \cdots \times U_{y_1, y}(x_\perp). \quad (\text{A4})$$

In the large- k limit, each $U_{y_m, y_{m-1}}$ covers an infinitesimal piece of the total path with a fixed length $\Delta = y_m - y_{m-1}$. Because of the locality of Eq. (A3) in y , it is clear that there will be no contractions between different factors in this product. For an individual factor, however, we may expand and perform the normal ordering

$$\begin{aligned} U_{y_m, y_{m-1}}(x_\perp) &= \mathbf{1} + i \int_{y_{m-1}}^{y_m} dy \Lambda(y, x_\perp) + i^2 \int_{y_{m-1}}^{y_m} dy \int_y^{y_m} dy' \Lambda(y, x_\perp) \Lambda(y', x_\perp) + \mathcal{O}(\Delta^3) \\ &= : \mathbf{1} + i \int_{y_{m-1}}^{y_m} dy \Lambda(y, x_\perp) : + \mathbf{1} \left(i^2 \frac{g^4 N_c \gamma(0)}{2} \right) \int_{y_{m-1}}^{y_m} dy \mu^2(y, Q^2) + \mathcal{O}(\Delta^2), \end{aligned} \quad (\text{A5})$$

where we have kept all terms up to order Δ . This is the only nonsuppressed tadpole contribution if the function $\mu^2(y)$ is finite. As a consequence, we have

$$\begin{aligned} U_{y_m, y_{m-1}}(x_\perp) U_{y_{m-1}, y_{m-2}}(x_\perp) &= : \mathbf{1} + i \int_{y_{m-2}}^{y_m} dy \Lambda(y; x_\perp) : + \mathbf{1} \left(-\frac{g^4 N_c \gamma(0)}{2} \right) \int_{y_{m-2}}^{y_m} dy \mu^2(y, Q^2) + \mathcal{O}(\Delta^2) \\ &= : U_{y_m, y_{m-2}}(x_\perp) : \exp \left[\left(-\frac{g^4 N_c \gamma(0)}{2} \right) \int_{y_{m-2}}^{y_m} dy \mu^2(y, Q^2) \right], \end{aligned} \quad (\text{A6})$$

which immediately carries over to $U_{\infty, y}(x_\perp)$ upon insertion into Eq. (A4). The dangerous tadpole contributions therefore can be factored out from a link operator by writing it in the normal-ordered form. Using this result, we find

$$\begin{aligned}
G_{ij}(y, x_\perp; y', x'_\perp) &= \int_y^\infty dy' \int_{\bar{y}}^\infty d\bar{y}' \langle \{ U_{\infty, y'} [\nabla^i \Lambda(y')] U_{y', \infty} \} (x_\perp) : \{ U_{\infty, \bar{y}'} [\nabla^i \Lambda(\bar{y}')] U_{\bar{y}', \infty} \} (\bar{x}_\perp) : \rangle_\Lambda \\
&\quad \times \exp \left[\left(-\frac{g^4 N_c \gamma(0)}{2} \right) \left(\int_{\bar{y}'}^\infty + \int_{y'}^\infty \right) dy' \mu^2(y', Q^2) \right] \\
&= \int_y^\infty dy' \int_{\bar{y}}^\infty d\bar{y}' \tilde{G}_{ij}(y', x_\perp; \bar{y}', \bar{x}_\perp) \exp \left[\left(-\frac{g^4 N_c \gamma(0)}{2} \right) \left(\int_{y'}^\infty + \int_{\bar{y}'}^\infty \right) dy' \mu^2(y', Q^2) \right]. \quad (\text{A7})
\end{aligned}$$

The expectation value of the product of normal-ordered fields we dubbed \tilde{G} does not contain any contractions within the individual U 's. This is now easily evaluated order by order and then resummed. Expanding the U 's to zeroth order, we have

$$\begin{aligned}
\tilde{G}_{ij}^{ab0}(y', x_\perp; \bar{y}', \bar{x}_\perp) \\
= \delta^{ab} \delta(y' - \bar{y}') g^4 \mu^2(y', Q^2) \nabla_i \bar{\nabla}_j \gamma(x_\perp - \bar{x}_\perp). \quad (\text{A8})
\end{aligned}$$

In first order, a quick computation gives

$$\begin{aligned}
\tilde{G}_{ij}^{ab1}(y', x_\perp; \bar{y}', \bar{x}_\perp) &= \tilde{G}_{ij}^{ab0}(y', x_\perp; \bar{y}', \bar{x}_\perp) (-g^4) (-N_c) \\
&\quad \times \gamma(x_\perp - \bar{x}_\perp) \int_{y'}^{y^0} dy'' \mu^2(y'', Q^2). \quad (\text{A9})
\end{aligned}$$

In this equation, N_c is the number of colors.

Similarly, in n th order, we find

$$\begin{aligned}
\tilde{G}_{ij}^{abn}(y', x_\perp; \bar{y}', \bar{x}_\perp) &= \frac{(g^4)^n N_c^n \gamma(x_\perp - \bar{x}_\perp)}{n!} \\
&\quad \times \left[\int_{y'}^\infty dy'' \mu^2(y'', Q^2) \right]^n \\
&\quad \times \tilde{G}_{ij}^{ab0}(y', x_\perp; \bar{y}', \bar{x}_\perp). \quad (\text{A10})
\end{aligned}$$

Summing up, multiplying the tadpole factors, and then performing the remaining y' and \bar{y}' integrations now allows us to write an explicit expression in which the leading infrared divergence cancel. Assuming $y > \bar{y}$, the result is

$$\begin{aligned}
G_{ij}^{ab}(y, x_\perp; y', x'_\perp) \\
= -\delta^{ab} (\nabla_i \bar{\nabla}_j' \gamma(x_\perp - x'_\perp)) \frac{1}{N_c [\gamma(x_\perp - x'_\perp) - \gamma(0)]} \\
\times (1 - \exp\{g^4 N_c \chi(y, Q^2) [\gamma(x_\perp - x'_\perp) - \gamma(0)]\}), \quad (\text{A11})
\end{aligned}$$

where we have defined

$$\chi(y, Q^2) = \int_y^\infty dy' \mu^2(y', Q^2). \quad (\text{A12})$$

The quantity $\chi(y, Q^2)$ is the total charge squared per unit area at rapidity greater than the rapidity y .

APPENDIX B: THE EIKONALIZED PROPAGATOR

In this appendix, we will derive an expression for the vector field propagator in the eikonal approximation. We will solve the equation of motion for the hard fluctuation field in the presence of an external soft vector potential. Throughout this analysis we neglect the effects of the classical background field.

We start with the transverse component of the Yang-Mills equations,

$$D_\mu F^{\mu i} = 0, \quad (\text{B1})$$

and write the total field A_μ as

$$A_\mu = \delta A_\mu + s_\mu,$$

where δA_μ is the hard field describing the fluctuations with high longitudinal momentum and s_μ is the soft field with small longitudinal momenta only.

We assume that the only large momentum in the problem is the longitudinal momentum of the hard field δA_i . Therefore, in the equation of motion for the hard field, we keep only those terms which involve derivatives of the hard field with respect to x^- , the coordinate conjugate to large momentum p^+ . The equation of motion for the hard field then becomes

$$\partial^- \partial_- \delta A_i - i[s^-, \partial_- \delta A_i] = D^-(s) \partial_- \delta A_i = 0. \quad (\text{B2})$$

To calculate the propagator we need to find eigenfunctions of the operator $D^-(s) \partial_-$. In order to do this, we write

$$\delta A_i^\lambda(x) = e^{ipx} \tilde{\delta A}_i^\lambda(x),$$

where the eigenvalue $\lambda = p^2$ and $\tilde{\delta A}_i$ is a slowly varying function of x^- . Then eigenvalue equation becomes

$$D^-(s) \tilde{\delta A}_i(x) = 0,$$

which has the solution

$$\begin{aligned}
\tilde{\delta A}_{i,\alpha}^{a,\lambda}(x, p) &= \left[\hat{\mathbf{P}} \exp \left(-i \int_{-\infty}^{x^+} dz^+ s^-(z^+, x^-, x_t) \right) \right]_{ac} \\
&\quad \times \epsilon_i^{(\lambda)}(p) \otimes u_{(\alpha)}^c, \quad (\text{B3})
\end{aligned}$$

where a is the color label, λ is the eigenvalue index, and $\epsilon_i^{(\lambda)}$ and $u_{(\alpha)}$ are the polarization vector and color basis vector, respectively. The eigenfunctions, therefore, are

$$\delta A_{i,\alpha}^{a,\lambda}(x,p) = \left[\hat{\mathbf{P}} \exp \left(-i \int_{-\infty}^{x^+} dz^+ s^-(z^+, x^-, x_t) \right) \right]_{ac} \times \epsilon_i^{(\lambda)}(p) \otimes u_{(\alpha)}^c e^{ipx}. \quad (\text{B4})$$

The propagator is constructed as

$$G_{ij}^{ab}(x,y) = \int d\lambda \frac{\delta A_i^{a,\lambda}(x) \delta A_j^{\dagger b,\lambda}(y)}{\lambda - i\epsilon}.$$

Since the soft field s is a slowly varying function of x^- , we can neglect its variation with x^- and write it as a function of z^- where $z^- \sim (x^- + y^-)$ is the average $(-)$ coordinate associated with the soft field. The expression for the propagator can be written as

$$G_{ij}^{ab}(x,y) = \delta_{ij} \delta^2(x_t - y_t) \int \frac{dp^+ dp^-}{(2\pi)^2} \times \frac{e^{-ip^+(x^- - y^-)} e^{-ip^-(x^+ - y^+)}}{-2p^+ p^- - i\epsilon} \times \left[\hat{\mathbf{P}} \exp \left(-i \int_{y^+}^{x^+} dz^+ s^-(z^+, x^-, x_t) \right) \right]_{ab}. \quad (\text{B5})$$

Here we have used

$$p^2 = -2p^+ p^- + p_t^2 \approx -2p^+ p^-$$

and

$$\sum_{\lambda} \epsilon_i^{(\lambda)}(p) \epsilon_j^{(\lambda)}(p) \otimes \sum_{\alpha} u_{(\alpha)}^c u_{(\alpha)}^d = -\delta_{ij} \delta^{cd}.$$

The integration over p^- is straightforward and gives a factor proportional to $\theta(x^+ - y^+)$ for positive p^+ . To get the propagator in momentum space, we Fourier transform with respect to relative and center-of-mass coordinates $x^- - y^-$ and $z^- \sim (x^- + y^-)$ to get

$$G_{ij}^{ab}(K^+, k^+, x^+, y^+, x_t, y_t) = \frac{i}{2} \delta_{ij} \delta^2(x_t - y_t) \theta(x^+ - y^+) \frac{1}{K^+} \times \left[\hat{\mathbf{P}} \exp \left(-i \int_{y^+}^{x^+} dz^+ s^-(z^+, k^+, x_t) \right) \right]_{ab}, \quad (\text{B6})$$

where K^+ and k^+ are the momenta conjugate to $(x^- - y^-)$ and $(x^- + y^-)$, respectively. For negative K^+ we get the same expression above with the argument of the θ function switched around and a relative minus sign.

-
- [1] E. A. Kuraev, L. N. Lipatov, and V. S. Fadin, *Sov. Phys. JETP* **45**, 199 (1977); Ya. Ya. Balitsky and L. N. Lipatov, *Sov. J. Nucl. Phys.* **28**, 22 (1978).
- [2] L. McLerran and R. Venugopalan, *Phys. Rev. D* **49**, 2233 (1994); **49**, 3352 (1994); **50**, 2225 (1995).
- [3] A. H. Mueller, *Nucl. Phys.* **B307**, 34 (1988); **B317**, 573 (1989); **B335**, 115 (1990).
- [4] K. Geiger and B. Mueller, *Nucl. Phys.* **B369**, 600 (1992); *Phys. Rep.* **258**, 237 (1995).
- [5] J. D. Bjorken, *Phys. Rev. D* **27**, 140 (1983).
- [6] A. Kovner, L. McLerran, and H. Weigert, *Phys. Rev. D* **52**, 3809 (1995).
- [7] A. Ayala-Mercado, J. Jalilian-Marian, L. McLerran, and R. Venugopalan, *Phys. Rev. D* **52**, 2935 (1995); **53**, 458 (1996).
- [8] R. V. Gavai and R. Venugopalan, *Phys. Rev. D* **54**, 5795 (1996).
- [9] Yuri V. Kovchegov, *Phys. Rev. D* **54**, 5463 (1996).
- [10] L. V. Gribov, E. M. Levin, and M. G. Ryskin, *Phys. Rep.* **100**, 1 (1983).
- [11] S. Catani, F. Fiorani, and G. Marchesini, *Nucl. Phys.* **B336**, 18 (1990); S. Catani, F. Fiorani, G. Marchesini, and G. Oriani, *ibid.* **B361**, 645 (1991).
- [12] O. Nachtmann, *Ann. Phys. (N.Y.)* **209**, 436 (1991).
- [13] A. H. Mueller, *Nucl. Phys.* **B415**, 373 (1994).
- [14] Yu. L. Dokshitzer, V. A. Khoze, A. H. Mueller, and S. I. Troyan, *Basics of Perturbative QCD* (Editions Frontières, Gif-sur-Yvette, 1991).